CMST 31(1–3) 33–47 (2025) DOI:10.12921/cmst.2025.0000012

Stability Analysis of Three Coupled Kerr Oscillators: Implications for Quantum Computing

K. Chmielewski[1], **K. Grygiel**[2*], **K. Bartkiewicz**[2]

[1] *Adam Mickiewicz University*
Faculty of Physics and Astronomy
61-614 Poznań, Poland

[2] *Adam Mickiewicz University*
Department of Quantum Information, Faculty of Physics and Astronomy
61-614 Poznań, Poland
[*] *E-mail: grygielk@amu.edu.pl*

Received: 27 June 2025; accepted: 22 July 2025; published online: 18 August 2025

Abstract: We investigate the classical dynamics of optical nonlinear Kerr couplers, focusing on their potential relevance to quantum computing applications. The system consists of three Kerr-type nonlinear oscillators arranged in two configurations: a triangular arrangement, where each oscillator is coupled to the others, and a sandwich arrangement, where only the middle oscillator interacts with the two outer ones. The system is driven by an external periodic field and subject to dissipative processes. Its evolution is governed by six non-autonomous differential equations derived from a Kerr Hamiltonian with nonlinear coupling terms. We demonstrate that even for identical Kerr media, the interplay between nonlinear couplings and mismatched fundamental and pump frequencies gives rise to rich and complex dynamics, including the emergence of multiple stable attractors. These attractors are highly sensitive to both the coupling configuration and initial conditions. A key contribution of this work is a detailed stability analysis based on numerical calculation of Lyapunov exponents, revealing transitions from regular to chaotic dynamics as damping is reduced. We identify critical damping thresholds for the onset of chaos and characterize phenomena such as chaotic beats. These findings offer insights for potential experimental realizations and are directly relevant to emerging quantum technologies, where Kerr parametric oscillators play a central role in quantum gates, error correction protocols, and quantum neural network architectures.

Key words: Kerr oscillators, Lyapunov exponents, quantum technology, chaotic beats

I. Introduction

Nonlinear optical systems based on the Kerr effect have emerged as a key area of overlap between classical nonlinear dynamics and quantum information science. Extensive research on such systems has explored both the classical [1, 2] and quantum [3–6] properties of the generated optical fields, offering valuable insights into fundamental physical processes and enabling a range of practical applications (as briefly reviewed in Sec. II). In particular, systems of coupled oscillators with Kerr-type nonlinearity have garnered significant interest due to their rich dynamical behavior and potential applications in optical signal processing, all-optical switching, and, more recently, quantum information processing.

The nonlinear Kerr effect, characterized by an intensity-dependent refractive index, facilitates self-phase modulation and enables complex interactions when multiple optical fields are coupled. In systems of coupled Kerr oscillators, this nonlinearity gives rise to a wide spectrum of dynamical behaviors, from regular periodic motion to intricate chaotic dynamics. This richness makes such systems valu-

able both for advancing theoretical understanding and for enabling diverse technological applications. Recent progress in nanophotonics and integrated optics has significantly improved the feasibility of experimentally realizing these systems (see [7] and references therein). Notably, silicon nitride microresonators have demonstrated high-efficiency optical parametric oscillation, achieving conversion efficiencies of up to 29% [8].

A particularly significant development is the recent emergence of Kerr parametric oscillators (KPOs) as promising building blocks for quantum processors, especially in superconducting circuit platforms [6, 9, 10]. Over the past few years (2022–2025), these systems have demonstrated key advantages, including high gate fidelities, enhanced error resilience, and increased computational capabilities [11]. The extension from two to three coupled oscillators – the central focus of this work – represents a critical threshold, enabling quantum functionalities unattainable in simpler configurations. Three-oscillator systems exhibit significantly richer phase-space structures, supporting up to eight stable fixed points under specific parameter regimes [12], thereby offering an expanded state space for quantum information encoding and manipulation.

The mathematical description of three coupled KPOs in the quantum regime involves a Hamiltonian comprising multiple nonlinear interaction terms:

$$H = \sum_{i=1}^{3}\left[\Delta_i a_i^\dagger a_i - \frac{K_i}{2}(a_i^\dagger a_i)^2 + \frac{p_i}{2}(a_i^2 + a_i^{\dagger 2})\right] + + \sum_{i,j>i}^{3} J_{ij}(a_i^\dagger a_j + a_i a_j^\dagger), \quad (1)$$

where Δ_i denotes the detuning frequency, K_i the Kerr nonlinearity strength, p_i the pumping amplitude, and J_{ij} the coupling strength between oscillators. While this Hamiltonian formulation applies to the few-photon quantum regime, our classical analysis offers complementary insights into the system's behavior in higher-excitation regimes, particularly concerning stability, multistability, and the onset of chaos.

In the commercial sector, quantum computing platforms based on coupled nonlinear oscillators are beginning to take shape. A notable example is IBM's Quantum System Two, launched in 2023, which introduced the first modular quantum computer featuring three coupled Heron processors. This architecture supports the execution of up to 1800 quantum gates within coherence times – nearly quadrupling the capacity of earlier systems [10]. Such advances highlight the growing importance of a detailed understanding of multi-oscillator Kerr systems, from both theoretical and practical perspectives.

Earlier work by Śliwa and Grygiel [13] explored the dynamics of two coupled Kerr oscillators, uncovering rich phase-space structures characterized by multiple coexisting attractors and transitions between regular and chaotic behavior. Building on their findings, the present study extends the framework to three coupled oscillators, introducing additional degrees of freedom and novel coupling topologies. These extensions give rise to significantly more intricate dynamical behavior, enabling the exploration of new stability regimes and potential applications in quantum information processing.

It is also worth highlighting previous fully quantum-mechanical treatments of triple Kerr oscillator couplers. Notably, Kalaga et al. [14] demonstrated that such a system can function as a nonlinear quantum scissors device and effectively operate as a three-qubit model. More recently, Hanapi et al. [15] investigated an optical coupler composed of three second-harmonic generation systems, focusing on the generation of nonclassical optical fields. However, these studies primarily concentrated on quantum aspects. In contrast, our present work emphasizes the classical regime, particularly through a detailed stability analysis using Lyapunov exponents – an approach that, to our knowledge, has not yet been applied to systems of three coupled Kerr oscillators.

The study of chaotic dynamics in nonlinear optical systems holds both fundamental and practical importance. On a fundamental level, it sheds light on the mechanisms governing the transition from regular to chaotic behavior in complex nonlinear systems. From a practical perspective, controlled chaos has been proposed for diverse applications, including secure optical communication [16], high-speed random number generation [17], and photonic reservoir computing [18].

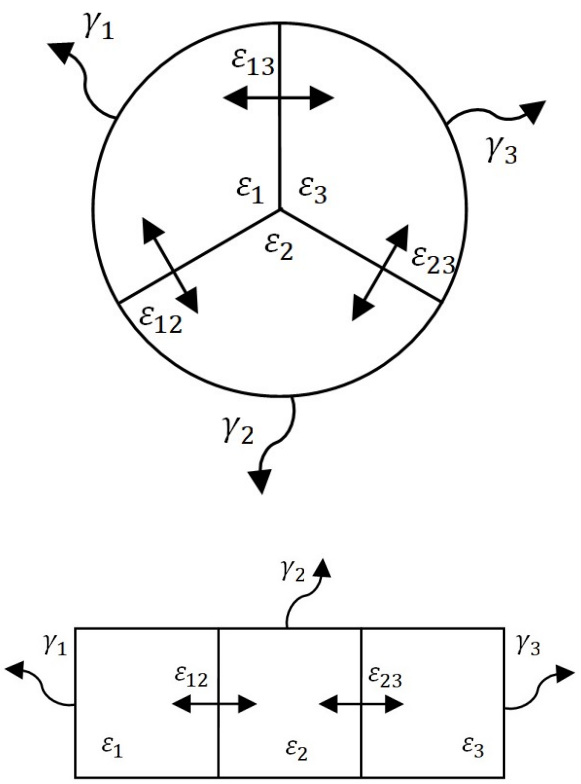

Fig. 1. Cross-sections of two coupling configurations: the triangular arrangement (top), in which all three oscillators are mutually coupled; and the sandwich arrangement (bottom), where the middle oscillator is coupled to both outer oscillators, while the first and third have no direct coupling

This paper builds upon previous research by systematically analyzing the dynamics and stability of three coupled Kerr oscillators under various coupling configurations. Our primary focus is on the influence of nonlinear couplings on system stability and phase-space evolution, with particular attention to the onset of chaos as key parameters are varied.

The novel contributions of our study include: (1) a comparative analysis of both triangular and sandwich coupling topologies (Fig. 1); (2) a comprehensive Lyapunov exponent analysis identifying transitions to chaotic regimes; (3) the discovery of multiple coexisting stable attractors with distinct phase-space structures dependent on coupling parameters, along with a mapping of their basins of attraction; and (4) the demonstration of signal patterns known as chaotic beats, generated by the system under specific conditions.

Before introducing our model and presenting its numerical solutions, we first highlight the significance of the optical Kerr effect in contemporary quantum nonlinear physics.

II. On the Fundamental and Practical Role of the Optical Kerr Effect

Although this paper focuses on the classical Kerr model, the underlying phenomena are highly relevant to quantum technologies due to their fundamental significance and wide range of applications.

The optical Kerr effect plays a central role in quantum state engineering and quantum information processing (QIP), attracting sustained interest due to its rich nonlinear dynamics and broad applicability across various platforms in quantum optics and related fields. These include cavity quantum electrodynamics (QED) [4], circuit QED (based on superconducting quantum circuits coupled to microwave resonators) [6, 9], atom optics (using Rydberg atoms, cold atomic gases, and Bose-Einstein condensates) [19], as well as cavity optomechanical systems (see, e.g., [20, 21]). Moreover, Kerr-type systems serve as prototypical models for exploring chaotic dynamics and nonlinear quantum control, which are the central focus of this paper.

A qubit – whether a natural or artificial atom such as a superconducting circuit – dispersively coupled to a resonator (e.g., transmission line resonator) provides a versatile platform for exploring Kerr-type light-matter interactions. In this dispersive limit, the qubit induces measurable frequency and phase shifts in the resonator's spectrum, enabling effective Kerr nonlinearities. This approach is widely employed to realize Kerr-type interactions, particularly when the qubit-resonator (i.e., light-matter) coupling reaches the strong, ultrastrong, or even deep-strong regimes [22, 23].

The Kerr effect, which induces an intensity-dependent refractive index, gives rise to a variety of nonlinear optical phenomena, including dispersive optical bistability [5], self-focusing and self-phase modulation [24]. It also plays a central role in quantum light control by enabling photon blockade – an effect that suppresses the absorption of multiple photons, thereby allowing for the generation of single photons [25, 26]. This effect has been demonstrated in numerous experiments (see [6, 27] for references). Beyond single-photon blockade, the Kerr effect enables a wide range of advanced phenomena, such as multi-photon blockade [28–30]; nonreciprocal [31] and chiral [32] photon blockade effects; phonon blockade, in which mechanical excitations (phonons) are suppressed [33]; and hybrid photon-phonon blockade [34]. Photon [35, 36] and phonon [37] blockade effects in coupled Kerr oscillator systems have also been investigated as mechanisms for generating maximally entangled states, such as Bell states. Further studies of two coupled Kerr oscillators have led to the prediction of unconventional photon blockade [38], including its nonreciprocal variant [39], where even very weak Kerr nonlinearities can enable high-fidelity single-photon generation.

Beyond enabling the generation of Fock and Bell states via photon blockade, Kerr nonlinearity serves as a versatile resource for producing a broad spectrum of nonclassical states of light [40]. For example, it enables the creation of highly squeezed states [41–44], as well as macroscopically distinguishable quantum superpositions of coherent states, including the celebrated Schrödinger cat states [45, 46] and their multi-component analogs, often referred to as Schrödinger kitten states [47], which were experimentally realized in [48–50].

The Kerr effect is also fundamental to implementing quantum gates and performing quantum nondemolition (QND) measurements, where it facilitates the indirect observation of quantum states without destroying them [3, 51, 52], as demonstrated in several landmark experiments (see [19] for details). Among the various proposals for Kerr-based quantum gates (see, e.g., [11, 53, 54] and references therein), a particularly notable example is the implementation of fault-tolerant multi-qubit geometric entangling gates using photonic cat states generated by N Kerr nonlinear oscillators coupled to a common harmonic resonator [55]. That Kerr-based proposal is arguably superior to other quantum gate implementations based on bosonic codes (see Tab. 1 in [55]), offering higher gate fidelities and less demanding coherence requirements in terms of energy relaxation time (T_1) and dephasing time (T_2).

Many of these applications critically depend on achieving strong Kerr nonlinearity at the few-photon level. Various strategies have been proposed and experimentally explored to enhance this nonlinearity. In addition to the methods demonstrated in, e.g., Refs. [48–50], a particularly noteworthy approach involves the sequential application of two-photon squeezing processes – governed by the second-order nonlinear susceptibility $\chi^{(2)}$ – to systems with initially weak Kerr nonlinearity, which arises from the third-order susceptibility $\chi^{(3)}$ [23, 56]. This method enables, at least theoretically, an exponential enhancement of the Kerr nonlinearity.

These capabilities make the Kerr effect indispensable for both fundamental studies in nonlinear optics and the development of practical quantum technologies.

III. Model and Its Dynamics

The dynamics of a system comprising three coupled Kerr oscillators extends the two-oscillator model previously an-

alyzed in [13]. Introducing a third oscillator, coupled nonlinearly and operating at a distinct frequency, enriches the system's behavior and is governed by the following Hamiltonian:

$$H = H_0 + H_1 + H_2, \tag{2}$$

where

$$H_0 = \sum_{j=1}^{3} \omega_j a_j^* a_j + \frac{1}{2} \sum_{j=1}^{3} \epsilon_j (a_j^*)^2 a_j^2, \tag{3}$$

$$H_1 = \epsilon_{12} a_1^* a_2^* a_1 a_2 + \epsilon_{13} a_1^* a_3^* a_1 a_3 + \epsilon_{23} a_2^* a_3^* a_2 a_3, \tag{4}$$

$$H_2 = \mathrm{i} \sum_{j=1}^{3} \left[F_j \left(a_j^* e^{-\mathrm{i}\Omega_{jp} t} - a_j e^{\mathrm{i}\Omega_{jp} t} \right) \right]. \tag{5}$$

The Hamiltonian H_0 describes three independent Kerr oscillators, where ω_j denote their natural frequencies and ϵ_j quantify the strength of the Kerr nonlinearities. The term H_1 accounts for nonlinear interactions between oscillator pairs, with ϵ_{12}, ϵ_{13}, and ϵ_{23} representing the respective coupling strengths. Finally, H_2 captures the interaction of each oscillator with external driving fields, where F_j are the driving amplitudes and Ω_{jp} the corresponding pump frequencies.

The equations of motion for the complex variables a_1, a_2, and a_3 are derived from the Hamiltonian via the relation:

$$\dot{a}_j = -\mathrm{i} \frac{\partial H}{\partial a_j^*} - \gamma_j a_j, \tag{6}$$

where the final term accounts for dissipation, with γ_j denoting the damping rates. Thus, we obtain:

$$\begin{aligned} \frac{da_1}{dt} &= -\mathrm{i}\omega_1 a_1 - \mathrm{i}\epsilon_1 a_1^* a_1^2 - \mathrm{i}\epsilon_{12} a_1 a_2^* a_2 + \\ &\quad -\mathrm{i}\epsilon_{13} a_1 a_3^* a_3 + F_1 e^{-\mathrm{i}\Omega_{1p} t} - \gamma_1 a_1, \end{aligned} \tag{7}$$

$$\begin{aligned} \frac{da_2}{dt} &= -\mathrm{i}\omega_2 a_2 - \mathrm{i}\epsilon_2 a_2^* a_2^2 - \mathrm{i}\epsilon_{12} a_2 a_1^* a_1 + \\ &\quad -\mathrm{i}\epsilon_{23} a_2 a_3^* a_3 + F_2 e^{-\mathrm{i}\Omega_{2p} t} - \gamma_2 a_2, \end{aligned} \tag{8}$$

$$\begin{aligned} \frac{da_3}{dt} &= -\mathrm{i}\omega_3 a_3 - \mathrm{i}\epsilon_3 a_3^* a_3^2 - \mathrm{i}\epsilon_{23} a_3 a_2^* a_2 + \\ &\quad -\mathrm{i}\epsilon_{13} a_3 a_1^* a_1 + F_3 e^{-\mathrm{i}\Omega_{3p} t} - \gamma_3 a_3. \end{aligned} \tag{9}$$

The coupled nonlinear differential equations (7)–(9) define a six-dimensional dynamical system when decomposed into the real and imaginary parts of each complex variable a_j ($j = 1, 2, 3$), representing the optical field in each section of the coupler. For each oscillator, the evolution depends on its intrinsic frequency, Kerr nonlinearity, nonlinear coupling to the other oscillators, external driving forces, and energy dissipation.

The damping terms $-\gamma_j a_j$ are essential to our stability analysis, as they characterize energy dissipation within the system. These terms critically influence whether the system settles into periodic oscillations or evolves into chaotic dynamics. For specific parameter regimes, the equations admit periodic solutions of the form:

$$a_1(t) = \frac{F_1}{\gamma_1} \exp\left[-\mathrm{i} \left(\omega_1 + \epsilon_1 \frac{F_1^2}{\gamma_1^2} + \epsilon_{12} \frac{F_2^2}{\gamma_2^2} + \epsilon_{13} \frac{F_3^2}{\gamma_3^2} \right) t \right], \tag{10}$$

$$a_2(t) = \frac{F_2}{\gamma_2} \exp\left[-\mathrm{i} \left(\omega_2 + \epsilon_2 \frac{F_2^2}{\gamma_2^2} + \epsilon_{12} \frac{F_1^2}{\gamma_1^2} + \epsilon_{23} \frac{F_3^2}{\gamma_3^2} \right) t \right], \tag{11}$$

$$a_3(t) = \frac{F_3}{\gamma_3} \exp\left[-\mathrm{i} \left(\omega_3 + \epsilon_3 \frac{F_3^2}{\gamma_3^2} + \epsilon_{23} \frac{F_2^2}{\gamma_2^2} + \epsilon_{13} \frac{F_1^2}{\gamma_1^2} \right) t \right], \tag{12}$$

only if the pumping frequencies satisfy:

$$\begin{aligned} \Omega_{1p} &= \omega_1 + \epsilon_1 \frac{F_1^2}{\gamma_1^2} + \epsilon_{12} \frac{F_2^2}{\gamma_2^2} + \epsilon_{13} \frac{F_3^2}{\gamma_3^2}, \\ \Omega_{2p} &= \omega_2 + \epsilon_2 \frac{F_2^2}{\gamma_2^2} + \epsilon_{12} \frac{F_1^2}{\gamma_1^2} + \epsilon_{23} \frac{F_3^2}{\gamma_3^2}, \\ \Omega_{3p} &= \omega_3 + \epsilon_3 \frac{F_3^2}{\gamma_3^2} + \epsilon_{23} \frac{F_2^2}{\gamma_2^2} + \epsilon_{13} \frac{F_1^2}{\gamma_1^2}, \end{aligned} \tag{13}$$

and the initial conditions are:

$$a_{j0} = a_j(t = 0) = \frac{F_j}{\gamma_j}, \quad \text{where} \quad j = 1, 2, 3. \tag{14}$$

In phase space, these periodic solutions satisfy the following equations:

$$|a_j|^2 = \frac{F_j^2}{\gamma_j^2}. \tag{15}$$

For our analysis, we focus on a system with the following parameters: $\omega_1 = 1$, $\omega_2 = 0.5$, $\omega_3 = 0.25$, $\epsilon_1 = \epsilon_2 = \epsilon_3 = 0.01$, $F_1 = F_2 = F_3 = 5$, $\gamma_1 = = \gamma_2 = \gamma_3 = 0.5$, $\Omega_{1p} = 2.2$, $\Omega_{2p} = 1.7$, $\Omega_{3p} = 1.45$, and $\epsilon_{12} = \epsilon_{13} = \epsilon_{23} = 0.001$ (triangular configuration). With these parameters, the oscillators trace circular trajectories in phase space, each with a radius of 10, and oscillate at frequencies of 2.2, 1.7, and 1.45, respectively.

The coupling configurations we examine correspond to distinct arrangements of the three oscillators, as illustrated in Fig. 1. In the triangular arrangement, each oscillator is directly coupled to the other two, forming a fully connected network. In contrast, the sandwich arrangement features the middle oscillator coupled to both outer oscillators, with no direct interaction between the outer pair. These distinct topologies give rise to markedly different dynamics and stability characteristics. Notably, these coupling schemes have

direct analogues in quantum computing architectures, where specific coupling geometries can be engineered to realize targeted computational functionalities – for example, in the design of fiber couplers.

Furthermore, the system is six-dimensional and governed by 18 parameters. Exhaustively exploring all parameter combinations is practically infeasible. Consequently, it is necessary to focus on a carefully selected subset of parameters and thoroughly analyze the system's behavior within this reduced parameter space.

IV. Phase-Space Trajectories and Attractor Structure

The phase-space analysis of the system (7)–(9) reveals key dynamical properties. For initial conditions $a'_{j0} = = \operatorname{Re} a_{j0} = 10$ and $a''_{j0} = \operatorname{Im} a_{j0} = 0$ ($j = 1, 2, 3$), the phase points of all three subsystems follow circular trajectories of radius 10, as described by equations (10)–(12), with frequencies $\Omega_{1p} = 2.2$, $\Omega_{2p} = 1.7$, and $\Omega_{3p} = 1.45$. However, when the initial condition of the first subsystem is varied – while keeping $a'_{j0} = 10$ and $a''_{j0} = 0$ fixed for $j = 2, 3$ – multiple attractors emerge.

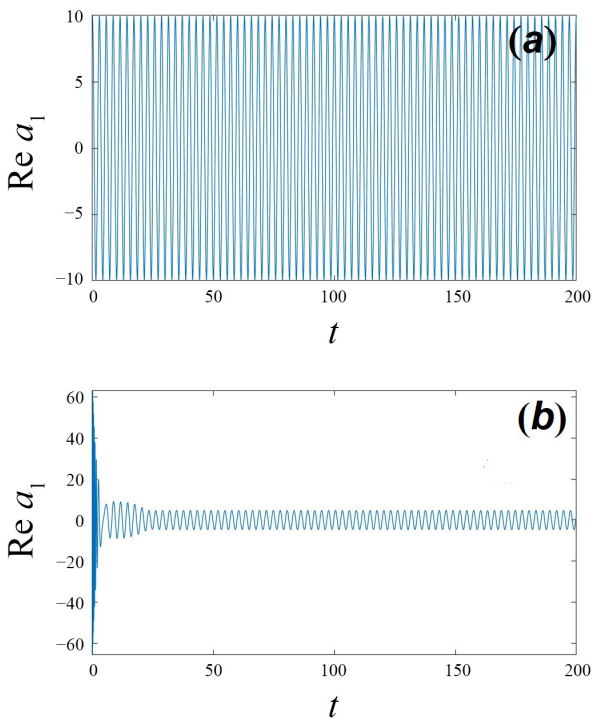

Fig. 2. Time evolution of $\operatorname{Re}(a_1(t))$ for the first oscillator subsystem, with parameters: $\omega_1 = 1$, $\omega_2 = 0.5$, $\omega_3 = 0.25$; $\epsilon_1 = = \epsilon_2 = \epsilon_3 = 0.01$; $F_1 = F_2 = F_3 = 5$; $\gamma_1 = \gamma_2 = \gamma_3 = 0.5$; $\Omega_{1p} = 2.2$, $\Omega_{2p} = 1.7$, $\Omega_{3p} = 1.45$; and coupling strengths $\epsilon_{12} = \epsilon_{13} = \epsilon_{23} = 0.001$ (triangular configuration). Initial conditions: (a) $\operatorname{Re} a_{j0} = 10$ and $\operatorname{Im} a_{j0} = 0$ for $j = 1, 2, 3$; (b) $\operatorname{Re} a_{10} = 48$, $\operatorname{Im} a_{10} = -48$, $\operatorname{Re} a_{20} = 10$, $\operatorname{Im} a_{20} = 0$, $\operatorname{Re} a_{30} = 10$, $\operatorname{Im} a_{30} = 0$

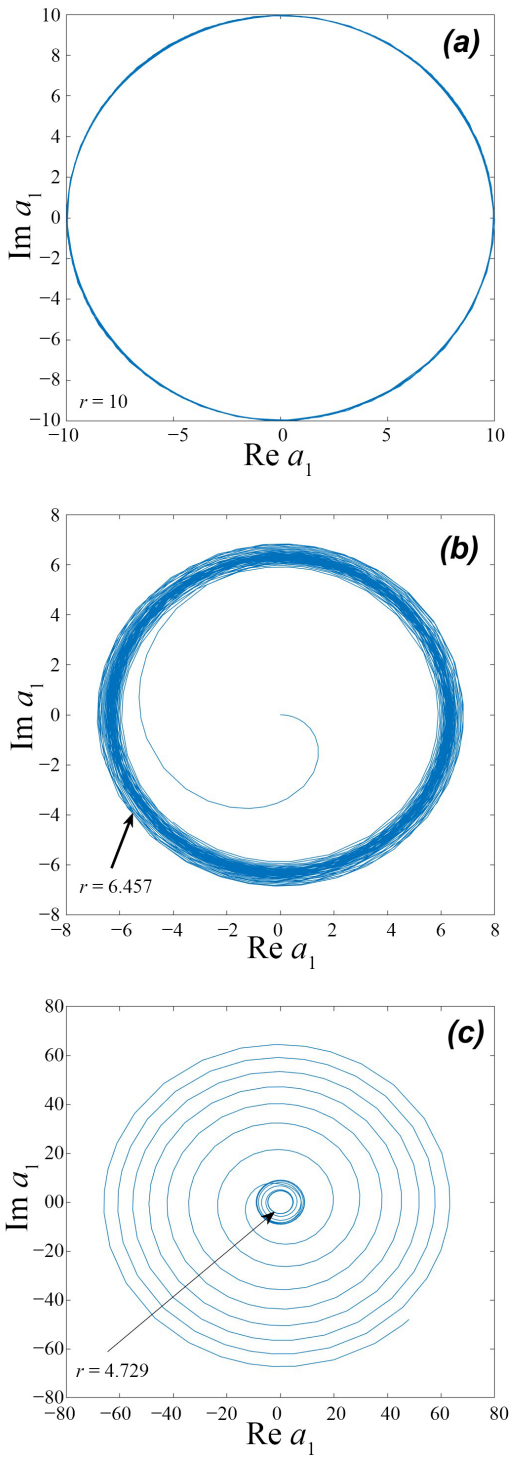

Fig. 3. Phase-space trajectories of the first Kerr oscillator with parameters as in Fig. 2, under the triangular configuration and varying initial conditions: (a) $\operatorname{Re} a_{10} = 10$, $\operatorname{Im} a_{10} = 0$, $\operatorname{Re} a_{20} = 10$, $\operatorname{Im} a_{20} = 0$, $\operatorname{Re} a_{30} = 10$, $\operatorname{Im} a_{30} = 0$; (b) $\operatorname{Re} a_{10} = 0$, $\operatorname{Im} a_{10} = 0$, $\operatorname{Re} a_{20} = 10$, $\operatorname{Im} a_{20} = 0$, $\operatorname{Re} a_{30} = 10$, $\operatorname{Im} a_{30} = 0$; (c) $\operatorname{Re} a_{10} = 48$, $\operatorname{Im} a_{10} = -48$, $\operatorname{Re} a_{20} = 10$, $\operatorname{Im} a_{20} = 0$, $\operatorname{Re} a_{30} = 10$, $\operatorname{Im} a_{30} = 0$. The trajectories demonstrate convergence toward three distinct attractors with radii: $r = 10$, $r' = = 6.457$, and $r'' = 4.729$, respectively

To systematically investigate this behavior, we performed numerical simulations in which the initial conditions were varied while the system parameters were fixed. A fourth-order Runge-Kutta method with adaptive step-size control was used to ensure both numerical stability and accuracy. Integration was carried out up to $t > 1000$ (in normalized units) to allow transient dynamics to decay and to reliably capture the system's asymptotic behavior.

First, we present the time evolution of the first Kerr oscillator – specifically, the real part of $a_1(t)$ – for the triangular arrangement. Fig. 2(a) shows the purely periodic behavior of the oscillator when the initial conditions $(\mathrm{Re}\, a_{10}, \mathrm{Im}\, a_{10})$ lie on the attractor (i.e., the limit cycle) of radius 10. When the initial conditions are outside the attractor, transient effects occur before the system reaches it (as shown in Fig. 2(b) – in this case, the attractor has a radius of 4.729).

A similar analysis to that shown in Fig. 2 reveals that the phase point representing the first subsystem eventually converges to one of three distinct circular attractors:

- the primary attractor, with $|a_1|^2 = 10^2$ (radius $r = = 10$),
- the secondary attractor, with $|a_1|^2 = (6.457)^2$ (radius $r' = 6.457$),
- the tertiary attractor, with $|a_1|^2 = (4.729)^2$ (radius $r'' = 4.729$).

Fig. 3(a) shows the phase point starting from initial conditions $\mathrm{Re}\, a_{10} = 10$, $\mathrm{Im}\, a_{10} = 0$, converging to the primary attractor with radius $r = 10$ by time $t = 150$. Fig. 3(b) illustrates convergence to the secondary attractor (radius $r' = = 6.457$) from the initial conditions $\mathrm{Re}\, a_{10} = 0$, $\mathrm{Im}\, a_{10} = = 0$. In Fig. 3(c), the phase point beginning at $\mathrm{Re}\, a_{10} = 48$, $\mathrm{Im}\, a_{10} = -48$ converges to the tertiary attractor (radius $r'' = 4.729$). In the context of quantum computing, these distinct stable states can correspond to different computational states in a multi-state quantum memory.

The basins of attraction for each attractor were mapped by sampling a grid of initial conditions in the $(\mathrm{Re}\, a_{10}, \mathrm{Im}\, a_{10})$ plane, as shown in Fig. 4. We observed that the basin boundaries exhibit fractal-like structures, reflecting a high sensitivity to initial conditions – a hallmark of nonlinear systems with multiple attractors.

Tab. 1. Attractor radii and frequencies for different coupling configurations, specifically the triangular arrangement ($\epsilon_{12} = \epsilon_{13} = = \epsilon_{23} = 0.001$) and the sandwich arrangement ($\epsilon_{13} = 0$, $\epsilon_{12} = = \epsilon_{23} = 0.001$)

Configuration	r	r'	r''	Ω_{1p}	Ω_{2p}	Ω_{3p}
triangular	10	6.457	4.729	2.2	1.7	1.45
sandwich	10	6.73	5.339	2.1	1.7	1.35

To investigate the influence of coupling configuration, we compared the triangular arrangement with the sandwich configuration, in which $\epsilon_{13} = 0$, meaning there is no direct coupling between the first and third oscillators. Tab. 1 summarizes the properties of the attractors for each configuration.

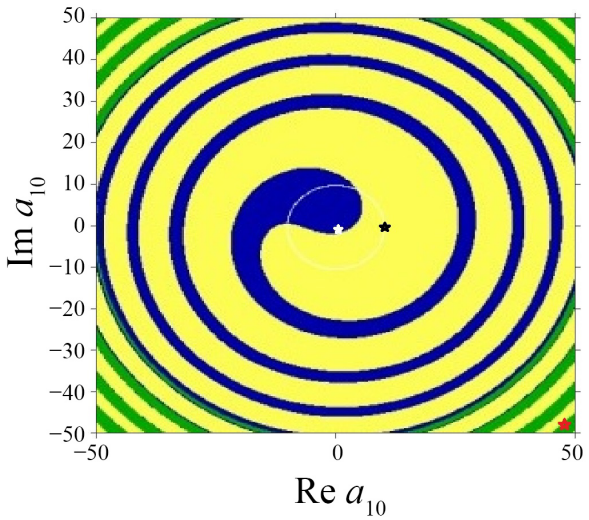

Fig. 4. Basin of attraction corresponding to the case shown in Fig. 3. Colors indicate which stable attractor the subsystem consisting of the first oscillator reaches from each initial condition $(\mathrm{Re}\, a_{10}, \mathrm{Im}\, a_{10})$: $r = 10$ (yellow), $r = 6.457$ (blue), and $r = = 4.729$ (green). Asterisks mark the exact initial conditions used in Fig. 3(a–c). Note that only the attractor with radius $r = 10$ is explicitly labeled in the figure

While both configurations exhibit similar transient behavior and ultimately converge to circular periodic orbits, one notable difference emerges: the sandwich configuration produces larger secondary and tertiary attractors than the triangular one. This counterintuitive finding suggests that reducing the number of couplings can, in certain cases, enhance rather than suppress the intensity of specific oscillation modes – highlighting the intricate and complex nature of nonlinear interactions in the system. Notably, reducing the number of couplings introduces greater asymmetry into the system, which may play a significant role in shaping the dynamical properties of the coupler. This finding has important implications for designing quantum computing architectures, where tailored coupling geometries can be engineered to achieve desired computational properties.

V. Lyapunov Exponent Analysis and Transition to Chaos

Lyapunov exponents offer a rigorous means of characterizing the stability of a dynamical system by quantifying the rate at which nearby trajectories in phase space diverge or converge. A positive maximal Lyapunov exponent indicates exponential divergence of initially close trajectories – a hallmark of chaotic behavior. In contrast, a zero maximal exponent corresponds to quasiperiodic dynamics, while a negative maximal exponent implies periodic behavior, where trajectories remain bounded and converge. The method applied ranks Lyapunov exponents in descending order. If the largest exponent is positive, the system is chaotic. If two or more ex-

ponents are positive, the system is classified as hyperchaotic, exhibiting even more complex instability.

In quantum computing applications, understanding the stability characteristics of Kerr oscillator systems is crucial for designing reliable quantum operations, as chaos can lead to information loss and decoherence.

For our system of three nonlinearly coupled Kerr oscillators, we employed the method of Wolf et al. [57], which incorporates the Gram-Schmidt reorthonormalization (GSR) algorithm. This method tracks the evolution of perturbation vectors in the tangent space alongside the phase-space trajectory, periodically reorthonormalizing the basis vectors to avoid numerical instability and ensure accurate computation of Lyapunov exponents.

The system of equations (7)–(9) defines a six-dimensional dynamical system. Linearizing around a reference trajectory yields an additional set of 36 variational equations – corresponding to six perturbation vectors in six-dimensional space – required to compute the full Lyapunov spectrum. Consequently, analyzing the three-oscillator Kerr coupler involves solving a total of 42 coupled ordinary differential equations (ODEs).

Our numerical implementation involved the following steps:

1. Simultaneous integration of the original system defined by Eqs. (7)–(9) along with the corresponding set of linearized variational equations.
2. Periodic application of the GSR procedure, typically every 0.01 time units, to maintain numerical stability of the tangent space vectors.
3. Accumulation of logarithmic rates of expansion and contraction along each orthonormal direction in phase space.
4. Long-time averaging of the accumulated rates, typically over more than 5000 time units, to ensure convergence and eliminate transient effects.

To ensure the robustness of our numerical procedure, we validated the results by confirming that the sum of all Lyapunov exponents approximates the theoretical expectation of $-(\gamma_1 + \gamma_2 + \gamma_3)$, which reflects the total dissipation in the system.

The identification of distinct stability regimes is particularly relevant for quantum computing applications, where controlled chaotic behavior can be leveraged for specific tasks such as random number generation and reservoir computing.

Given the system's high dimensionality and large parameter space, all Lyapunov spectrum calculations were performed using a fixed set of baseline parameters: $\omega_1 = 1$, $\omega_2 = 0.5$, $\omega_3 = 0.25$, $\epsilon_1 = \epsilon_2 = \epsilon_3 = 0.01$, $F_1 = = F_2 = F_3 = 5$, $\Omega_{2p} = 1.7$, and $\Omega_{3p} = 1.45$. The initial conditions were: $\mathrm{Re}\, a_{j0} = 10$, $\mathrm{Im}\, a_{j0} = 0$ $(j = 1, 2, 3)$. Fig. 5 presents the key results of our analysis of the Lyapunov exponent spectrum for the triangular configuration ($\epsilon_{12} = \epsilon_{13} = \epsilon_{23} = 0.001$), plotted as a function of the pumping frequency Ω_{1p} of the first Kerr oscillator. Each panel corresponds to a different value of the damping constants, with $\gamma_1 = \gamma_2 = \gamma_3 = \gamma$. Several critical observations emerge from this analysis:

1. **Strong damping regime** (Fig. 5(a) for $\gamma = 0.005$): All Lyapunov exponents remain negative and approximately constant across the entire frequency range, indicating a strongly dissipative regime. Here, the system consistently converges to stable fixed points or limit cycles, regardless of the pumping frequency. From a quantum computing perspective, such behavior corresponds to robust and predictable dynamics – essential for implementing high-fidelity quantum gates.
2. **Intermediate damping regime** (Fig. 5(b) for $\gamma = = 0.001$): Although all Lyapunov exponents remain negative and show similar variation across the pumping frequency range, there are more points of rapidly increasing exponents, indicating elevated sensitivity to parameter changes. The smaller magnitudes of the exponents imply much slower convergence to attractors. This regime may be advantageous for applications that benefit from heightened sensitivity to inputs, such as quantum sensing.
3. **Weak damping regime** (Fig. 5(c) for $\gamma = 0.0002$): The largest Lyapunov exponents approach zero at specific frequencies, indicating proximity to critical transitions. The spectrum exhibits pronounced frequency dependence, with fluctuations reflecting competing dynamical regimes. A detailed analysis reveals frequent quasi-periodic states. Similar "edge-of-chaos" regimes have been exploited in recent quantum neural network implementations to enhance computational capacity.
4. **Undamped regime** (Fig. 5(d) for $\gamma = 0$): A critical transition occurs in this regime, where some Lyapunov exponents become positive within specific frequency intervals, confirming the onset of chaotic behavior. These chaotic regimes are interspersed with regular (non-chaotic) windows, exhibiting intermittency – a hallmark of many nonlinear systems that can be harnessed for chaos-based computing applications. Moreover, the presence of extensive frequency ranges in Ω_{1p} supporting hyperchaotic dynamics underscores the system's potential usefulness for cryptographic applications and secure communications.

The transition to chaos as damping decreases can be understood as a competition between energy dissipation and nonlinear energy transfer combined with external pumping. When damping is sufficiently strong, energy dissipation dominates, suppressing nonlinear mode interactions and maintaining stable system behavior. As damping weakens, nonlinear coupling and pumping effects gain prominence, facilitating nontrivial energy exchanges that can lead to chaotic dynamics once dissipation is no longer able to contain them. In the context of quantum hardware, this insight is valuable for designing dissipation engineering strategies aimed either at preserving system stability or deliberately inducing controlled chaos for specialized applications.

A similar stability analysis was performed for the sandwich configuration shown in Fig. 1 (with $\epsilon_{13} = 0$). Under parameters analogous to those in Fig. 5, the system exhibits comparable behavior, as illustrated in Fig. 6. Notably, the

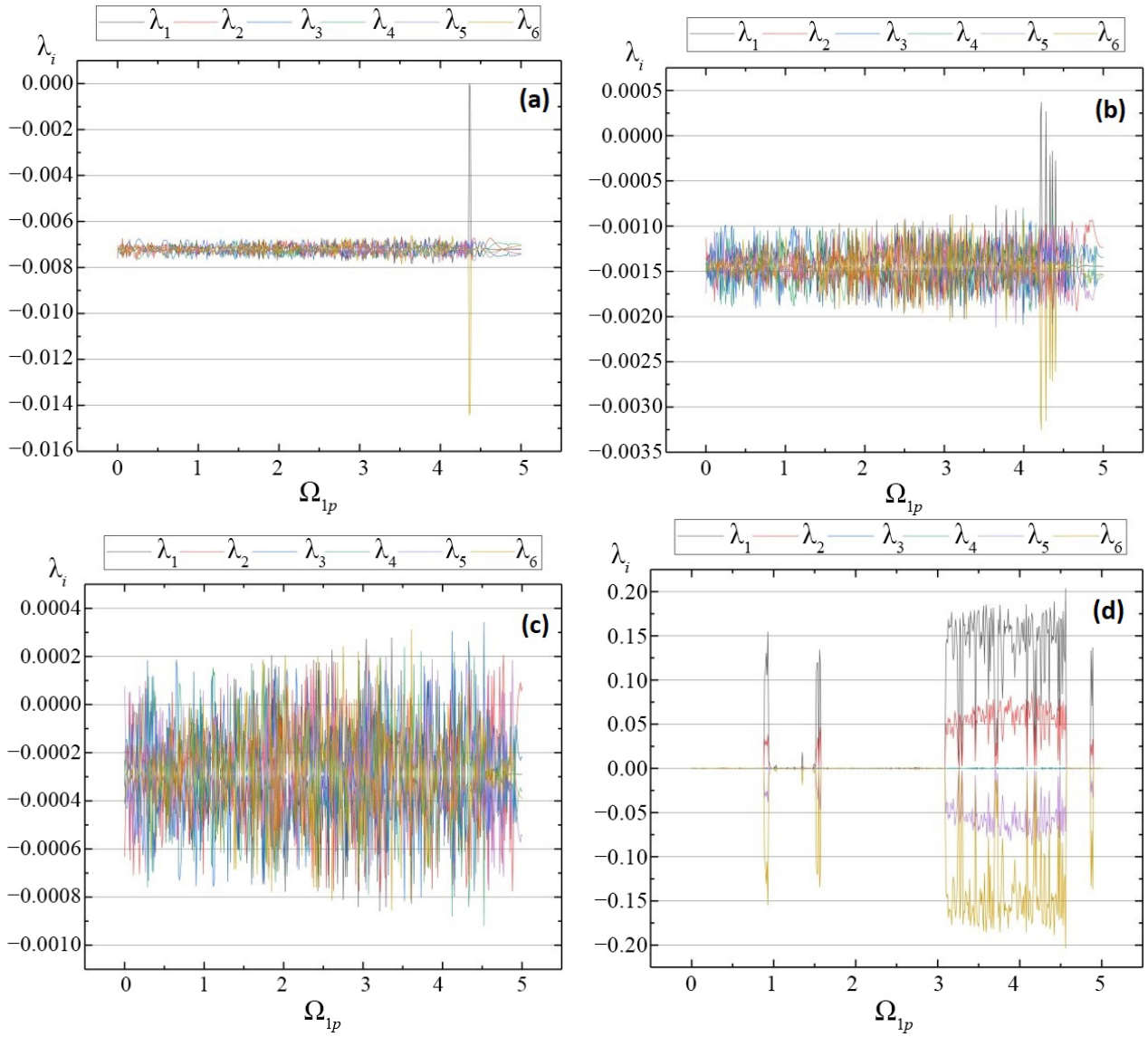

Fig. 5. Lyapunov exponents λ_1–λ_6 for the triangular arrangement ($\epsilon_{12} = \epsilon_{13} = \epsilon_{23} = 0.001$) of the Kerr couplers, shown as a function of the pumping frequency Ω_{1p} of the first oscillator for different damping constants: (a) $\gamma_1 = \gamma_2 = \gamma_3 = \gamma = 0.005$, (b) $\gamma = 0.001$, (c) $\gamma = 0.0002$, (d) $\gamma = 0$. Other system parameters are the same as in Fig. 2. Note the qualitative change in system behavior as damping decreases: in panel (d), the emergence of positive Lyapunov exponents signals the onset of chaotic – and potentially hyperchaotic – dynamics

regions of chaos and hyperchaos expand in the absence of damping, reflecting reduced overall stability. This decreased stability arises from increased asymmetry of the system: in the sandwich arrangement, the central Kerr oscillator couples to both neighbors, whereas each outer oscillator is coupled to only one neighbor.

To confirm that the observed chaotic behavior is genuine and not a numerical artifact, we performed several validation tests:

- Varying the integration step size and GSR intervals to verify numerical convergence.
- Testing multiple sets of initial conditions to ensure consistent Lyapunov spectra across simulations.
- Calculating the correlation dimension, which confirmed the fractal nature of the attractors in the chaotic regimes.

Furthermore, we investigated how the transition to chaos depends on the coupling strengths. We found that increasing the coupling parameters ϵ_{12}, ϵ_{13}, and ϵ_{23} lowers the critical damping threshold for chaos, confirming that nonlinear coupling is indeed the mechanism driving chaotic behavior. This effect is particularly pronounced in the sandwich configuration, highlighting the leading role of not only the coupling but also the asymmetry of the coupler system (Fig. 7). The Lyapunov exponents clearly indicate a marked increase in the system's instability (Fig. 7(d)). This finding is par-

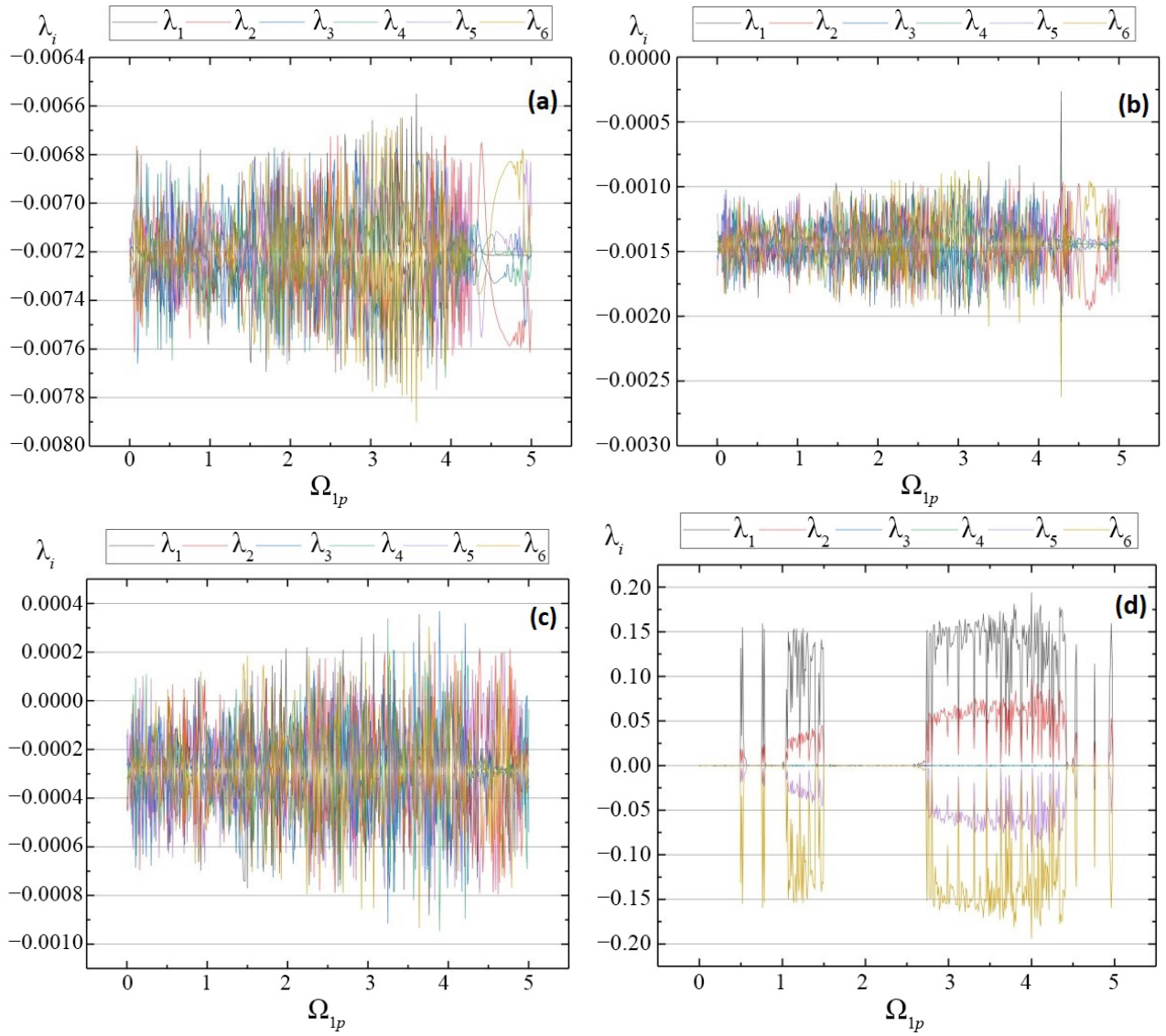

Fig. 6. Lyapunov exponents λ_1–λ_6 for the sandwich arrangement ($\epsilon_{13} = 0, \epsilon_{12} = \epsilon_{23} = 0.001$) of the Kerr couplers, shown as a function of the pumping frequency Ω_{1p} of the first oscillator for different damping constants: (a) $\gamma_1 = \gamma_2 = \gamma_3 = \gamma = 0.005$, (b) $\gamma = 0.001$, (c) $\gamma = 0.0002$, (d) $\gamma = 0$. Other system parameters are the same as in Fig. 2

ticularly relevant for quantum computing implementations, where coupling strengths can be precisely tuned to achieve desired stability characteristics.

VI. Chaotic Beats

In certain coupled nonlinear systems, a distinctive dynamical behavior known as chaotic beats can be observed. This phenomenon was first numerically identified in a system of two coupled Kerr and Duffing oscillators [58]. Since then, chaotic beats have been reported in various systems, including Chua's circuit [59], coupled second-harmonic generators of light [60], and memristive-driven Chua circuits [61]. Notably, the phenomenon has also been demonstrated experimentally in an electronic setup consisting of two forced dissipative LCR oscillators sharing a nonlinear element [62].

In general, chaotic beats refer to signals where the envelope of amplitude modulation exhibits chaotic fluctuations while the underlying carrier frequency remains nearly constant. This phenomenon typically arises in weakly coupled nonlinear systems. Interestingly, in a system of three coupled Kerr oscillators, we identified a specific set of parameters for which chaotic beats emerge even under strong coupling conditions. In this configuration, the intensity of the first oscillator, defined as $I_1(t) = |a_1(t)|^2$, evolves – after an initial period of strongly chaotic transients – into a regime of persistent, stationary-like chaotic beats, as illustrated in Fig. 8. Further analysis reveals that as the pumping frequency Ω_{1p} increases, the system gradually loses its beat-like character-

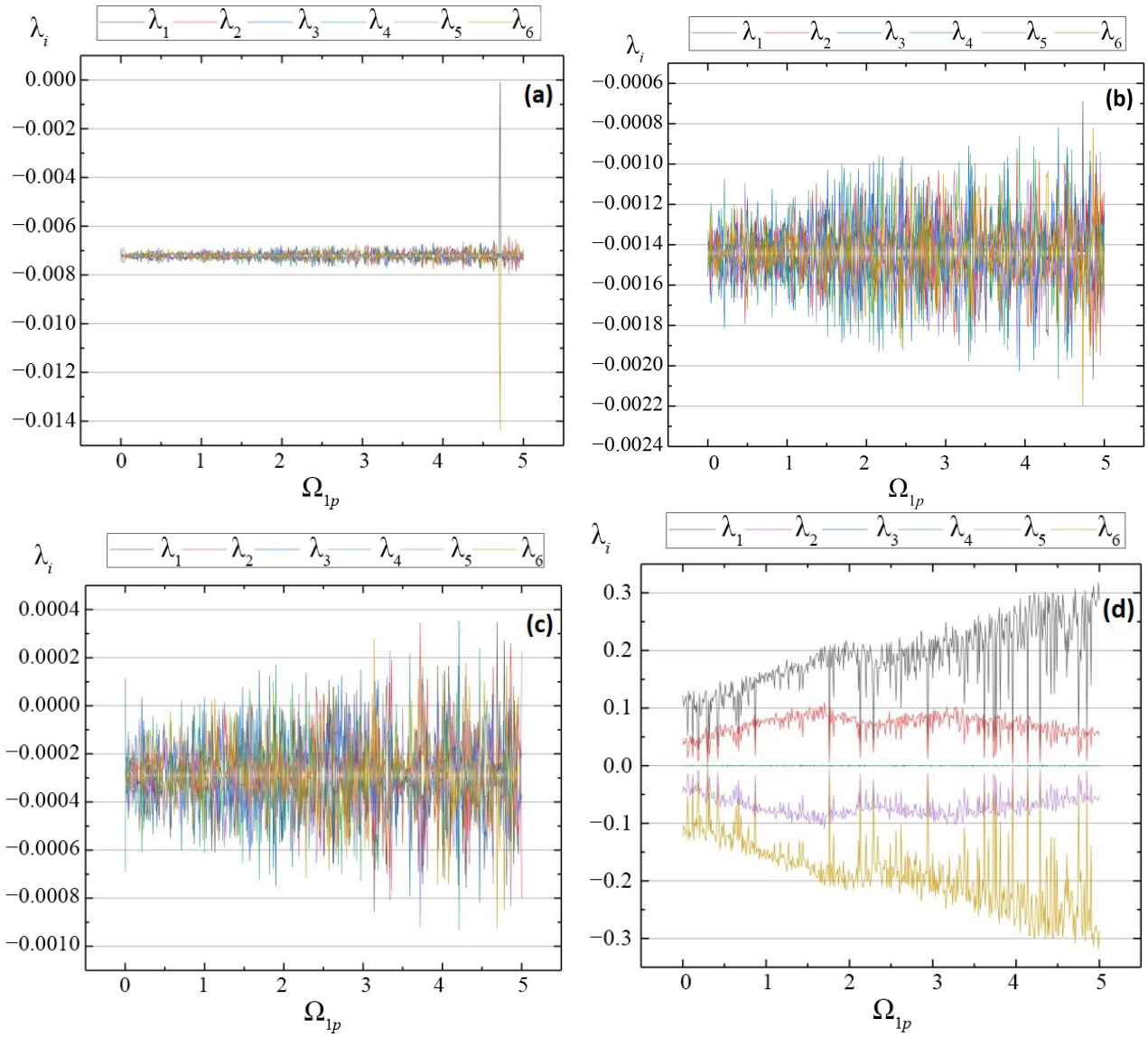

Fig. 7. Lyapunov exponents λ_1–λ_6 for the sandwich arrangement of the Kerr couplers under strong coupling conditions ($\epsilon_{13} = 0, \epsilon_{12} = = \epsilon_{23} = 0.01$), shown as a function of the pumping frequency Ω_{1p} of the first oscillator for different damping constants: (a) $\gamma_1 = \gamma_2 = = \gamma_3 = \gamma = 0.005$, (b) $\gamma = 0.001$, (c) $\gamma = 0.0002$, (d) $\gamma = 0$. Other system parameters are the same as in Fig. 2

istics and transitions into a regime of purely chaotic behavior.

VII. Quantum Computing Applications and Experimental Implementations

Our analysis of three coupled Kerr oscillators carries important implications for emerging quantum computing technologies. Although the present treatment is classical, the identified stability regimes remain highly relevant for mesoscopic and macroscopic systems where classical and quantum types of behavior coexist. In this section, we explore the connection between our results and recent advancements in quantum computing, particularly in the context of experimental platforms that utilize nonlinear oscillators and engineered dissipation.

VII. 1. Advantages of Three-Oscillator Systems

Three coupled Kerr oscillators represent a critical minimum configuration for several quantum computing applications that cannot be realized with simpler two-oscillator systems:

1. **Enhanced computational basis:** The multiple stable attractors identified (summarized in Tab. 1) provide an expanded state space for information encoding. In quantum computing implementations based on Kerr parametric oscillators (KPOs), these states can represent distinct computational basis states [12].
2. **Triangular coupling topology:** The triangular configuration enables genuine three-body interactions that cannot arise in systems with only two oscillators. Recent work by Margiani et al. [12] demonstrated that a system of three strongly coupled KPOs can function

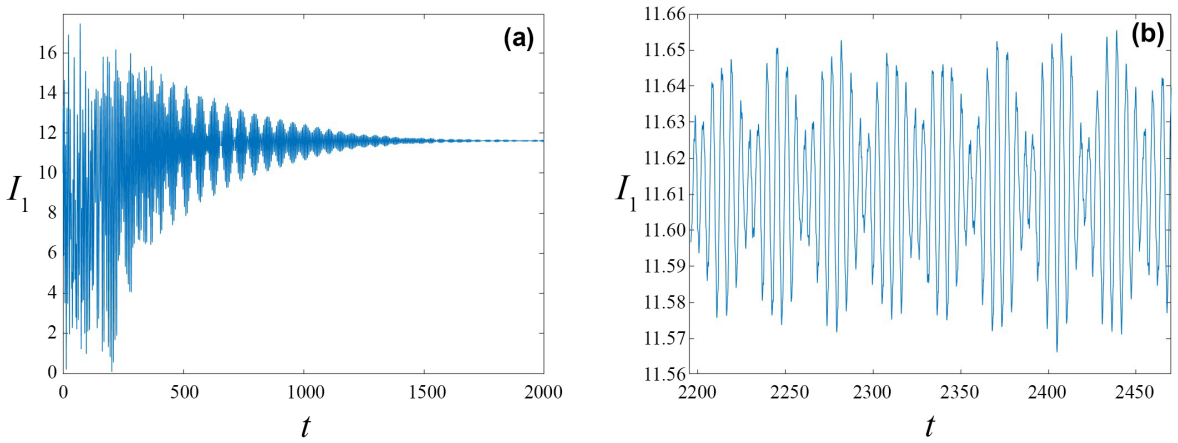

Fig. 8. Chaotic beats in the first Kerr oscillator. Time evolution of the intensity $I_1(t) = |a_1(t)|^2$ is shown for strong coupling in the sandwich configuration, with pumping frequency $\Omega_{1p} = 1$. All other parameters are the same as in Fig. 7(d). Panel (a) illustrates the initial strongly chaotic transient regime, while panel (b) displays the subsequent emergence of a stationary chaotic beat pattern

as a Boltzmann machine capable of simulating Ising Hamiltonians. This architecture has direct applications in solving combinatorial optimization problems and highlights the computational potential of nonlinear oscillator networks.

3. **Error correction capabilities:** Systems composed of three coupled oscillators support redundant encoding schemes that enhance robustness against noise and decoherence – key requirements for scalable quantum computing. Our stability analysis identifies parameter regimes in which such error-resilient encoding is most effective, offering guidance for designing quantum architectures with improved fault tolerance.

VII. 2. Experimental Platforms

Recent experimental advances have made the implementation of coupled Kerr oscillator systems increasingly feasible:

1. **Superconducting circuits:** Superconducting circuits have emerged as a leading platform for realizing coupled Kerr parametric oscillators (KPOs) in quantum computing [6, 9]. Recent experiments have demonstrated high-fidelity quantum gate operations using KPOs, including R_x gates via parity-selective transitions [11], and two-qubit R_{zz} gates with fidelities exceeding 99.9% in systems of highly detuned KPOs [53].
2. **Integrated photonics:** Silicon nitride microresonators have demonstrated high-efficiency optical parametric oscillation with conversion efficiencies reaching 29% [8]. These platforms benefit from scalability and compatibility with existing semiconductor manufacturing technologies. For example, in situ control of integrated Kerr nonlinearity with a tuning range of 10 dB has recently been demonstrated [7], enabling dynamic modulation of nonlinear interactions in superconducting quantum circuits.
3. **Commercial implementations:** IBM's Quantum System Two, introduced in 2023, marks a significant milestone in the commercial advancement of quantum processors based on coupled nonlinear oscillators. The system is capable of executing up to 1800 quantum gates within coherence times – nearly quadrupling the capacity of previous-generation devices [10].

The critical damping thresholds identified in Sec. V offer valuable guidance for experimental implementations by delineating parameter regimes that ensure stable operation versus those prone to chaotic transitions. This insight is especially relevant for superconducting circuit platforms, where damping rates can be precisely engineered.

VII. 3. Potential Applications for Quantum Computing

The distinct dynamical regimes revealed by our Lyapunov exponent analysis correspond to specific operational modes with direct applications in quantum computing:

1. **Quantum gates:** The stable regime characterized by negative Lyapunov exponents is ideal for implementing reliable quantum gates. Recent experiments have demonstrated that KPOs can perform both high-fidelity single-qubit operations and entangling gates [11].
2. **Quantum neural networks:** The near-critical regime, where Lyapunov exponents approach zero yet remain negative (Fig. 5(c)), offers enhanced computational capacity well-suited for quantum neural networks. Recent studies have demonstrated that even with just two coupled quantum oscillators, a quantum reservoir containing up to 81 effective neurons can be realized, achieving 99% accuracy on benchmark tasks [18].
3. **Chaos-based computing:** The chaotic regime with positive Lyapunov exponents can be exploited for specialized computing tasks, including quantum random number generation and quantum cryptography. Controlled chaotic behavior in optical systems has been demonstrated as an effective mechanism for generating high-entropy random bit streams [17].

Our analysis of the impact of coupling configurations on attractor properties (Tab. 1) is particularly relevant for quantum computing applications requiring precise control over system dynamics. Notably, the observation that sandwich configurations support larger secondary and tertiary attractors suggests that deliberate removal of specific couplings can enhance particular computational functionalities.

VIII. Comparative Analysis and Future Work

VIII. 1. Comparison with Two-Oscillator Systems

Our three-oscillator system shares certain features with the two-oscillator case studied by Śliwa and Grygiel [13], including the presence of multiple attractors and parameter-dependent dynamics. However, the addition of a third oscillator gives rise to novel phenomena and richer dynamical behavior, including:

1. **Increased attractor complexity:** The three-oscillator system supports a more diverse set of attractors, including a tertiary attractor not observed in the two-oscillator case. This can be attributed to the additional degrees of freedom and coupling pathways.
2. **Configuration-dependent dynamics:** The triangular and sandwich configurations exhibit distinct dynamical properties. In particular, the sandwich configuration supports larger secondary and tertiary attractors, suggesting that in specific parameter regimes, reduced coupling can counterintuitively enhance intensity of the process.
3. **Lower chaos threshold:** Compared to the two-oscillator system, our three-oscillator configuration transitions to chaos at higher damping values, indicating increased dynamical complexity.

VIII. 2. Physical Mechanisms

The multiple attractors observed in our system arise from nonlinear mode competition. The nonlinear coupling terms in Eqs. (7)–(9) facilitate energy exchange between oscillators, creating a complex energy landscape with multiple local minima that correspond to distinct, stable oscillation patterns.

The transition to chaos as damping decreases reflects the delicate balance between energy dissipation and nonlinear energy transfer. When damping is sufficiently strong, dissipation dominates, yielding simple and stable attractor structures. As damping weakens, nonlinear energy transfer gains prominence, ultimately driving the system into chaotic dynamics once dissipation can no longer compensate for these nonlinear effects.

VIII. 3. Connection to Quantum-Classical Correspondence

While our analysis is classical, it provides insights into the behavior of quantum Kerr systems in the semiclassical regime, where photon numbers are large. Recent studies have established connections between classical Lyapunov exponents and quantum chaos indicators, such as out-of-time-ordered correlators (OTOCs) [63].

The stable attractors identified in our system correspond to coherent states in the quantum description, whereas the chaotic regions relate to situations where quantum states exhibit rapid entanglement growth and delocalization. This quantum-classical correspondence is particularly relevant for superconducting circuit implementations, which often operate in a mesoscopic regime where both classical and quantum effects are important.

VIII. 4. Limitations and Future Work

Several limitations of our current model should be acknowledged:

1. **Classical approximation:** Our analysis is entirely classical, neglecting quantum effects that may become significant at low field intensities or in specialized configurations designed to enhance quantum correlations.
2. **Simplified coupling:** The coupling terms in our model represent instantaneous interactions, omitting potential time delays and frequency-dependent effects that may occur in real optical systems.
3. **Parameter restrictions:** We have focused on symmetric configurations with identical oscillator parameters ϵ_j in order to isolate the effects of coupling topologies. However, allowing for asymmetric parameters could reveal additional, potentially richer dynamical behavior.

Future work may address these limitations by:

- Extending the model to include quantum effects, potentially revealing connections to quantum chaos.
- Investigating asymmetric configurations with varied oscillator parameters.
- Exploring the effects of time-delayed coupling, which may introduce additional complexity and could be relevant for applications such as reservoir computing.
- Developing control strategies to stabilize desired attractors or enable switching between attractors for use in optical routing applications.

IX. Conclusions

This paper has presented a comprehensive stability analysis of three coupled Kerr oscillators in both triangular and sandwich configurations, providing new insights into the dynamics of coupled nonlinear optical systems with significant implications in quantum computing. Using numerical simulations and Lyapunov exponent analysis, we have characterized the system's behavior across various parameter regimes, with particular focus on transitions from regular to chaotic dynamics.

Our key findings can be summarized as follows:

1. **Multiple stable attractors:** The subsystem consisting of the first oscillator exhibits three distinct circular attractors in phase space, each with a different radius and dependent on initial conditions. The complex basin structure of these attractors reveals the intricate nature of the underlying dynamics. In quantum computing implementations, these distinct states can serve

as computational basis states for information encoding.

2. **Configuration-dependent properties:** The coupling configuration (triangular vs. sandwich) significantly affects the attractor properties and system frequencies. Counterintuitively, the sandwich configurations, despite having fewer direct couplings, leads to larger secondary and tertiary attractors compared to the fully-coupled triangular arrangement. This finding has important implications for quantum hardware design, indicating that modifying coupling configurations can substantially enhance computational performance.
3. **Damping-controlled transition to chaos:** Lyapunov exponent analysis reveals a transition from stable to chaotic dynamics as damping decreases. We identify critical damping thresholds below which chaos emerges, with the undamped system ($\gamma = 0$) exhibiting fully developed chaos, as indicated by positive Lyapunov exponents. Understanding these stability characteristics is essential both for designing quantum operations with predictable performance and for applications that intentionally leverage chaos for computational advantage.
4. **Frequency-dependent stability windows:** Even in chaotic regimes, certain pumping frequencies support islands of stability, suggesting the possibility of controlling the system's behavior through careful parameter selection. This frequency dependence could be exploited for frequency-selective quantum operations or for implementing multi-frequency encoding schemes.
5. **Chaotic beats:** The system under consideration can generate characteristic signals known as chaotic beats. Unexpectedly, these were found in the regime of strong coupling of the three Kerr oscillators – whereas this phenomenon is typically associated with weakly coupled systems. The multitude of parameters and the resulting richness of dynamical behaviors suggest that this specific type of system dynamics can emerge across a wide range of coupler parameter configurations.

The significance of these results extends beyond the specific system studied here. The mechanisms of transition to chaos that we have identified – involving the competition between nonlinear coupling and dissipation – are likely applicable to a wide range of coupled nonlinear oscillator systems. Our findings on the impact of coupling topology on stability may inform the design of nonlinear optical devices where controlled chaos or switching between multiple stable states is desired.

In the context of quantum computing, our work contributes to the understanding of Kerr parametric oscillator systems, which are increasingly employed as fundamental building blocks in quantum processors. The stability analysis we have presented provides insights into parameter regimes suitable for implementing high-fidelity quantum gates, error-resilient encoding schemes, and specialized computing paradigms such as quantum neural networks.

Potential applications of these results include optical switches based on controlled transitions between attractors, secure communication systems leveraging chaotic dynamics, random number generation using the unpredictable nature of the chaotic regime, multi-state optical memory elements utilizing the system's multiple attractors, quantum gate implementations in superconducting circuit platforms, and error correction schemes exploiting the enhanced stability of specific parameter regimes.

Future research will focus on extending this analysis to asymmetric configurations, including time-delayed coupling effects, and developing experimental implementations to verify our theoretical predictions. Furthermore, investigating the quantum analogs of the classical dynamics explored in this study may reveal new phenomena at the quantum-classical boundary, particularly in the context of quantum chaos and its applications in quantum information processing.

Acknowledgment

The authors would like to express their gratitude to Prof. Adam Miranowicz for his valuable comments and careful reading of the final version of the manuscript. K.B. was supported by the Polish National Science Centre (NCN) under the Maestro Grant No. DEC-2019/34/A/ST2/00081.

References

[1] R.W. Boyd, *Nonlinear Optics*, Academic Press, Amsterdam (2008).
[2] Y.S. Kivshar, G.P. Agrawal, *Optical Solitons: From Fibers to Photonic Crystals*, Academic Press, San Diego (2003).
[3] M.O. Scully, M.S. Zubairy, *Quantum Optics*, Cambridge University Press, Cambridge, UK (1997).
[4] C. Gerry, P. Knight, *Introductory Quantum Optics*, Cambridge University Press, Cambridge (2006).
[5] D.F. Walls, G.J. Milburn, *Quantum Optics*, Springer, Berlin (2006).
[6] X. Gu, A.F. Kockum, A. Miranowicz, Y. Liu, F. Nori, *Microwave photonics with superconducting quantum circuits*, Phys. Rep. **718–719**, 1–102 (2017).
[7] C. Cui, L. Zhang, L. Fan, *In situ control of effective Kerr nonlinearity with Pockels integrated photonics*, Nat. Phys. **18**, 497–501 (2022).
[8] M. Perez, G. Moille, X. Lu, J. Stone, F. Zhou, K. Srinivasan, *High-performance Kerr microresonator optical parametric oscillation on a silicon chip*, Nature Commun. **14**, 242 (2023).
[9] Y. Yin, H. Wang, M. Mariantoni, R.C. Bialczak, R. Barends, Y. Chen, M. Lenander, E. Lucero, M. Neely *et al.*, *Dynamic quantum Kerr effect in circuit quantum electrodynamics*, Phys. Rev. A **85**, 023826 (2021).
[10] IBM, *IBM Debuts Next-Generation Quantum Processor & IBM Quantum System Two*, IBM Newsroom (2023).
[11] T. Kanao, S. Masuda, S. Kawabata, H. Goto, *Quantum Gate for a Kerr Nonlinear Parametric Oscillator Using Effective Excited States*, Phys. Rev. Applied **18**, 014019 (2022).
[12] G. Margiani, O. Ameye, O. Zilberberg, A. Eichler, *Three strongly coupled Kerr parametric oscillators forming a Boltzmann machine*, arXiv:2504.04254 (2025).
[13] I. Śliwa, K. Grygiel, *Periodic orbits, basins of attraction and chaotic beats in two coupled Kerr oscillators*, Nonlin. Dynam. **67**, 755–765 (2012).

[14] J.K. Kalaga, A. Kowalewska-Kudłaszyk, W. Leoński, A. Barasiński, *Quantum correlations and entanglement in a model comprised of a short chain of nonlinear oscillators*, Phys. Rev. A **94**, 032304 (2016).

[15] M.S.M. Hanapi, A-B.M.A. Ibrahim, R. Julius, P.K. Choudhury, H. Eleuch, *Nonclassical light in a three-waveguide coupler with second-order nonlinearity*, EPJ Quant. Techn. **11**, 51 (2024).

[16] G.D. Van Wiggeren, R. Roy, *Communication with Chaotic Lasers*, Science **279**, 1198–1200 (1998).

[17] A. Uchida, K. Amano, M. Inoue, K. Hirano, S. Naito, H. Someya, I. Oowada, T. Kurashige, M. Shiki, S. Yoshimori, K. Yoshimura, P. Davis, *Fast physical random bit generation with chaotic semiconductor lasers*, Nat. Photonics **2**, 728–732 (2008).

[18] D. Brunner, M.C. Soriano, C.R. Mirasso, I. Fischer, *Parallel photonic information processing at gigabyte per second data rates using transient states*, Nat. Commun. **4**, 1364 (2013).

[19] S. Haroche, J.M. Raimond, *Exploring the Quantum: Atoms, Cavities and Photons*, Oxford University Press, Oxford (2006).

[20] S. Aldana, C. Bruder, A. Nunnenkamp, *Equivalence between an optomechanical system and a Kerr medium*, Phys. Rev. A **88**, 043826 (2013).

[21] X. Wang, W. Qin, A. Miranowicz, S. Savasta, F. Nori, *Unconventional Cavity Optomechanics: Nonlinear Control of Phonons in the Acoustic Quantum Vacuum*, Phys. Rev. A **100**, 063827 (2019).

[22] A.F. Kockum, A. Miranowicz, S. Liberato, S. Savasta, F. Nori, *Ultrastrong coupling between light and matter*, Nat. Rev. Phys. **1**, 19 (2019).

[23] W. Qin, A.F. Kockum, C.S. Muñoz, A. Miranowicz, F. Nori, *Quantum amplification and simulation of strong and ultrastrong coupling of light and matter*, Phys. Rep. **1078**, 1 (2024).

[24] R. Tanaś, A. Miranowicz, Ts. Gantsog, *Quantum phase properties of nonlinear optical phenomena*, [In:] *Progress in Optics* **35**, Eds. E. Wolf, Elsevier, Amsterdam (1996), 355–446.

[25] W. Leoński, R. Tanaś, *Possibility of producing the onephoton state in a kicked cavity with a nonlinear Kerr medium*, Phys. Rev. A **49**, R20(R) (1994).

[26] A. Imamoğlu, H. Schmidt, G. Woods, M. Deutsch, *Strongly Interacting Photons in a Nonlinear Cavity*, Phys. Rev. Lett. **79**, 1467 (1997).

[27] W. Leoński, A. Kowalewska-Kudłaszyk, *Quantum Scissors: Finite-Dimensional States Engineering*, Prog. Opt. **56**, 131 (2011).

[28] A. Miranowicz, M. Paprzycka, Y. Liu, J. Bajer, F. Nori, *Two-photon and three-photon blockades in driven nonlinear systems*, Phys. Rev. A **87**, 023809 (2013).

[29] C. Hamsen, K.N. Tolazzi, T. Wilk, G. Rempe, *Two-Photon Blockade in an Atom-Driven Cavity QED System*, Phys. Rev. Lett. **118**, 133604 (2017).

[30] A. Kowalewska-Kudłaszyk, S.I. Abo, G. Chimczak, J. Peřina Jr., F. Nori, A. Miranowicz, *Two-photon blockade and photon-induced tunneling generated by squeezing*, Phys. Rev. A **100**, 053857 (2019).

[31] R. Huang, A. Miranowicz, J.-Q. Liao, F. Nori, H. Jing, *Nonreciprocal Photon Blockade*, Phys. Rev. Lett. **121**, 153601 (2018).

[32] Y. Zuo, Y.-F. Jiao, X.-W. Xu, A. Miranowicz, L.-M. Kuang, H. Jing, *Chiral photon blockade*, Opt. Express **32**, 22020–22030 (2024).

[33] Y.-X. Liu, A. Miranowicz, Y.B. Gao, J. Bajer, C.P. Sun, F. Nori, *Qubit-induced phonon blockade as a signature of quantum behavior in nanomechanical resonators*, Phys. Rev. A **82**, 032101 (2010).

[34] S. Abo, G. Chimczak, A. Kowalewska-Kudłaszyk, J. Peřina Jr., R. Chhajlany, A. Miranowicz, *Hybrid photon-phonon blockade*, Sci. Rep. **12**, 17655 (2022).

[35] W. Leoński, A. Miranowicz, *Kerr nonlinear coupler and entanglement*, J. Opt. B **6**, S37 (2004).

[36] A. Miranowicz, W. Leoński, *Two-mode optical state truncation and generation of maximally entangled states in pumped nonlinear couplers*, J. Phys. B **39**, 1683 (2006).

[37] A. Miranowicz, J. Bajer, N. Lambert, Y. Liu, F. Nori, *Tunable multiphonon blockade in coupled nanomechanical resonators*, Phys. Rev. A **93**, 013808 (2016).

[38] T.C.H. Liew, V. Savona, *Single Photons from Coupled Quantum Modes*, Phys. Rev. Lett. **104**, 183601 (2010).

[39] B. Li, R. Huang, X.-W. Xu, A. Miranowicz, H. Jing, *Nonreciprocal unconventional photon blockade in a spinning optomechanical system*, Photonics Res. **7**, 630–641 (2019).

[40] R. Tanaś, *Theory of Non-Classical States of Light*, [In:] V. Dodonov, V.I. Man'ko (Eds.), Taylor & Francis, London (2003).

[41] R. Tanaś, S. Kielich, *Self-squeezing of light propagating through nonlinear optically isotropic media*, Opt. Commun. **45**, 351 (1983).

[42] Y. Yamamoto, N. Imoto, S. Machida, *Amplitude squeezing in a semiconductor laser using quantum nondemolition measurement and negative feedback*, Phys. Rev. A **33**, 3243 (1986).

[43] R. Tanaś, A. Miranowicz, S. Kielich, *Squeezing and its graphical representations in the anharmonic oscillator model*, Phys. Rev. A **43**, 4014 (1991).

[44] J. Bajer, A. Miranowicz, R. Tanaś, *Limits of noise squeezing in Kerr effect*, Czech. J. Phys. **52**, 1313 (2002).

[45] B. Yurke, D. Stoler, *Generating quantum mechanical superpositions of macroscopically distinguishable states via amplitude dispersion*, Phys. Rev. Lett. **57**, 13 (1986).

[46] P. Tombesi, A. Mecozzi, *Generation of macroscopically distinguishable quantum states and detection by the squeezed-vacuum technique*, J. Opt. Soc. Am. B **4**, 1700 (1987).

[47] A. Miranowicz, R. Tanaś, S. Kielich, *Generation of discrete superpositions of coherent states in the anharmonic oscillator model*, Quantum Opt. **2**, 253 (1990).

[48] G. Kirchmair, B. Vlastakis, Z. Leghtas, S.E. Nigg, H. Paik, E. Ginossar, M. Mirrahimi, L. Frunzio, S.M. Girvin, R.J. Schoelkopf, *Observation of quantum state collapse and revival due to the single-photon Kerr effect*, Nature **495**, 205 (2013).

[49] X.L. He, Y. Lu, D.Q. Bao, H. Xue, W.B. Jiang, Z. Wang, A.F. Roudsari, P. Delsing, J.S. Tsai, Z.R. Lin, *Fast generation of Schrödinger cat states using a Kerr-tunable superconducting resonator*, Nat. Commun. **14**, 6358 (2023).

[50] D. Iyama, T. Kamiya, S. Fujii, H. Mukai, Y. Zhou, T. Nagase, A. Tomonaga, R. Wang, J.-J. Xue, S. Watabe, S. Kwon, J.-S. Tsai, *Observation and manipulation of quantum interference in a superconducting Kerr parametric oscillator*, Nat. Commun. **15**, 86 (2024).

[51] G.J. Milburn, D.F. Walls, *Quantum nondemolition measurements via quadratic coupling*, Phys. Rev. A **28**, 2065 (1983).

[52] N. Imoto, H.A. Haus, Y. Yamamoto, *Quantum nondemolition measurement of the photon number via the optical Kerr effect*, Phys. Rev. A **32**, 2287 (1985).

[53] H. Chono, T. Kanao, H. Goto, *Two-qubit gate using conditional driving for highly detuned Kerr-nonlinear parametric oscillators*, Phys. Rev. Research **4**, 043054 (2022).

[54] F.-F. Du, G. Fan, X.-M. Ren, *Kerr-effect-based quantum logical gates in decoherence-free subspace*, Quantum **8**, 1342 (2024).

[55] Y.-H. Chen, R. Stassi, W. Qin, A. Miranowicz, F. Nori, *Fault-tolerant multiqubit geometric entangling gates using photonic cat-state qubits*, Phys. Rev. Appl. **18**, 024076 (2022).

[56] M. Bartkowiak, L.-A. Wu, A. Miranowicz, *Quantum circuits for amplification of Kerr nonlinearity via quadrature squeezing*, J. Phys. B **47**, 145501 (2014).

[57] A. Wolf, J.B. Swift, H.L. Swinney, J.A. Vastano, *Determining Lyapunov exponents from a time series*, Physica D **16**, 285–317 (1985).

[58] K. Grygiel, P. Szlachetka, *Generation of chaotic beats*, Int. J. Bifurcation Chaos **12**, 635–644 (2002).

[59] D. Cafagna, G. Grassi, *A new phenomenon in nonautonomous Chua's circuits: Generation of chaotic beats*, Int. J. Bifurcation Chaos **14**, 1773–1788 (2004).

[60] I. Śliwa, P. Szlachetka, K. Grygiel, *Chaotic beats in a nonautonomous system governing second-harmonic generation of light*, Int. J. Bifurcation Chaos **17**, 3253–3257 (2007).

[61] A.I. Ahamed, K. Srinivasan, K. Murali, M. Lakshmanan, *Observation of chaotic beats in a driven memristive Chua's circuit*, Int. J. Bifurcation Chaos **21**, 737–757 (2011).

[62] M.P. Asir, A. Jeevarekha, P. Philominathan, *Experimental observation of chaotic beats in oscillators sharing nonlinearity*, Int. J. Bifurcation Chaos **26**, 1630027 (2016).

[63] J. Maldacena, S.H. Shenker, D. Stanford, *A bound on chaos*, J. High Energy Phys. **2016**, 106 (2016).

Kuba Chmielewski is a computer science student at the Faculty of Computing and Telecommunications, Poznan University of Technology, Poland. He graduated in 2020 with a BSc degree in physics from the Faculty of Physics and Astronomy, Adam Mickiewicz University, Poznań, Poland. His bachelor's thesis was supervised by Associate Professor Krzysztof Grygiel. His research interests include nonlinear dynamics, chaos, stability analysis of nonlinear systems using Lyapunov exponents, and nonlinear optics, especially in the context of optical couplers.

Krzysztof Grygiel is an Associate Professor at the Institute of Spintronics and Quantum Information, Faculty of Physics and Astronomy, Adam Mickiewicz University in Poznań, Poland. He completed his MSc in physics at the Faculty of Mathematics, Physics and Chemistry of Adam Mickiewicz University. He defended his PhD on the phenomenon of stimulated Raman scattering in 1988. His supervisor was Prof. Stanisław Kielich, founder and head of the Department of Nonlinear Optics, where he was employed after earning his doctorate and obtained his habilitation in 2002. His scientific activity has centered on the phenomena of classical and quantum chaos in optical systems, synchronization of chaotic systems, the dynamics of optical couplers, and the dynamics of molecular systems. He collaborated with the group of Prof. Jan Perina at Palacký University Olomouc, Czechia. From 2012 to 2020 he served as vice-dean of the Faculty of Physics and from 2017 to 2023, was head of the Department of Nonlinear Optics.

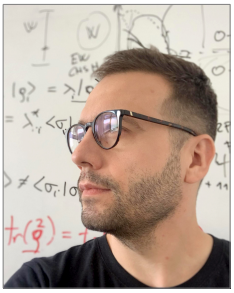

Karol Bartkiewicz is an Associate Professor at the Institute of Spintronics and Quantum Information, Faculty of Physics and Astronomy, Adam Mickiewicz University in Poznań, Poland. He earned his MSc in physics in 2008 and his PhD in 2012 from Adam Mickiewicz University under the supervision of Prof. Adam Miranowicz, followed by his habilitation in 2019. His research focuses on quantum physics, quantum optics, quantum information, and quantum machine learning, with over 1,600 citations to his work. Bartkiewicz leads research teams conducting experiments on quantum computers, exploring applications in quantum simulators, artificial intelligence, and optimization. His notable contributions include experimental demonstrations of temporal quantum steering, optimal quantum cloning for eavesdropping, and implementation of linear-optical quantum routers. He has collaborated extensively with institutions including Palacký University Olomouc, Czechia, and RIKEN. In 2024, he received the Award of the Minister of Science for outstanding teaching achievements. His current research interests include modeling complex quantum open systems and developing quantum machine learning algorithms, particularly generative such as QGAN and SQGEN.